



## Role of polyethylene glycol in electrodeposition of zinc–chromium alloys

T. AKIYAMA<sup>1</sup>, S. KOBAYASHI<sup>1</sup>, J. KI<sup>2</sup>, T. OHGAI<sup>2</sup> and H. FUKUSHIMA<sup>2</sup>

<sup>1</sup>Department of Industrial Chemistry, Faculty of Engineering, Kyushu Sangyo University, Fukuoka, Japan

<sup>2</sup>Department of Materials Process Engineering, Graduate School of Engineering, Kyushu University, Fukuoka, Japan

Received 14 April 1999; accepted in revised form 11 October 1999

**Key words:** polyethylene glycol, sulfate baths, Zn–Cr alloys

### Abstract

The role of polyethylene glycol (PEG) as an additive in the electrodeposition of zinc–chromium alloys was investigated in sulfate baths containing trivalent chromium. PEG with high molecular weight enabled the codeposition of metallic chromium with zinc, while chromium(III) was present in the deposits obtained from the baths containing PEG with lower molecular weight as well as the PEG-free bath. The polarization curves for the alloy deposition revealed that PEG with high molecular weight polarized the deposition potential of zinc to the reduction potential of chromium to permit the codeposition of chromium with zinc.

### 1. Introduction

The electrodeposition of zinc alloys on steel sheets has been developed to provide better corrosion resistances than the common zinc plating. The electroplating of zinc–iron and zinc–nickel alloys on steel strips is now being carried out on the commercial scale by steel manufacturers [1, 2]. Recently, attention has also been paid to a zinc–chromium alloy plated steel sheet because of its excellent properties for automotive body panels and electrical appliances. This plating process can be performed using sulfate solutions containing trivalent chromium ions [3–7].

In decorative single chromium plating, many attempts have been made to electroplate chromium from trivalent electrolytes, which are motivated by environmental deficiencies of the presently used hexavalent process [8–14]. However, it has been reported that the electroreduction behaviour of chromium(III) is atypical due to the complex nature of the chemistry and electrochemistry of chromium(III) species in the aqueous solutions [8, 9, 12, 15–20].

In zinc–chromium alloy plating, on the other hand, it is difficult to codeposit metallic chromium with zinc in simple sulfate electrolytes. The addition of certain types of polymers such as polyethylene glycol (PEG) to the electrolyte is essential to electroplate good quality zinc–chromium alloys [3–5]. In this work, the effect of PEG on the alloy deposition behaviour was investigated to clarify the role of PEG in the electrodeposition of zinc–chromium alloys.

### 2. Experimental details

#### 2.1. Electrolysis

An air sealed electrolytic cell was used for conducting the electrolysis at galvanostatic and coulometric (100 kC m<sup>-2</sup>) conditions. The cathode was copper and the anode platinum. For all experiments, the temperature was kept at 317 K and a saturated Ag/AgCl electrode was used as a reference.

Electrolytes were prepared by dissolving fixed amounts of high-grade reagents of ZnSO<sub>4</sub> (0.2 mol dm<sup>-3</sup>), Cr<sub>2</sub>(SO<sub>4</sub>)<sub>3</sub> (0.05 mol dm<sup>-3</sup>) and Na<sub>2</sub>SO<sub>4</sub> (0.2 mol dm<sup>-3</sup>) in distilled and deionized water. The bath pH was adjusted to 2.0 with sulfuric acid. Baths containing PEG of various mean molecular weights (200–30 000) were prepared with concentrations of 0, 0.1, 0.5, 1.0 and 5.0 g dm<sup>-3</sup>.

#### 2.2. Deposit analysis

Electrodeposited alloys were dissolved in aqua regia and both zinc and chromium in the deposits were quantitatively analysed by inductively coupled plasma spectrometry (ICP). Then the current efficiency and the composition of deposits were determined. Further, the partial current densities of zinc and chromium were calculated from the applied current density and the partial current efficiency of each metal to illustrate the polarization curve for the alloy deposition. Additionally, the chemical state of chromium in the deposits was estimated by X-ray photoelectron spectrometry (XPS). Scanning electron microscopy (SEM) was used to observe the morphology of the deposits.

### 3. Results and discussion

#### 3.1. Effect of PEG on alloy deposition

The effect of PEG concentration on the alloy deposition behaviour was studied in the bath containing PEG 1540. Figure 1(a) shows the current density-dependence of chromium content in the deposits obtained in the baths containing 0, 1.0 and 5.0 g dm<sup>-3</sup> of PEG. Regardless of the addition of PEG in the bath, the chromium content increased with increase in current density, while no codeposition of chromium was observed at current densities lower than 5 A dm<sup>-2</sup>. The current efficiency was extremely low at low current densities and massive deposition occurred only above 5 A dm<sup>-2</sup>. The chromium content of the deposits was higher in the PEG-containing baths than in the PEG-free baths. The chromium contents at 10 and 20 A dm<sup>-2</sup> were plotted against PEG concentration in the electrolytes and the results are shown in Fig. 1(b). A small addition of PEG enhanced the chromium content remarkably, although further increase in the chromium content was not

observed at higher PEG concentration than 1.0 g dm<sup>-3</sup>. This suggests that PEG adheres to the cathode layer and behaves as an adsorptive substance during the alloy deposition.

As mentioned above, the codeposition of chromium was observed even in the PEG-free baths, although PEG is effective to some extent in increasing the chromium content in the deposits. The chemical state of chromium in the deposits was determined by XPS. Figure 2 shows XPS spectra of chromium 3d 3/2 and 5/2 doublets in the deposits obtained in the PEG-free and PEG-containing (1 g dm<sup>-3</sup>) baths. As-plated specimens were argon sputtered for various duration to eliminate atmospherically oxidized and/or contaminated layer of the deposits.

The XPS spectra of the deposits from the PEG-free baths corresponded to that of chromium(III) after argon sputtering. Since the current efficiency for the zinc-chromium alloy deposition is about 80% at maximum, hydrogen evolves consistently to cause a pH rise in the cathode layer. On the other hand, chromium(III) aquo ions readily hydrolyse to form insoluble chromium(III) species at about pH 4. It is, therefore, suggested that

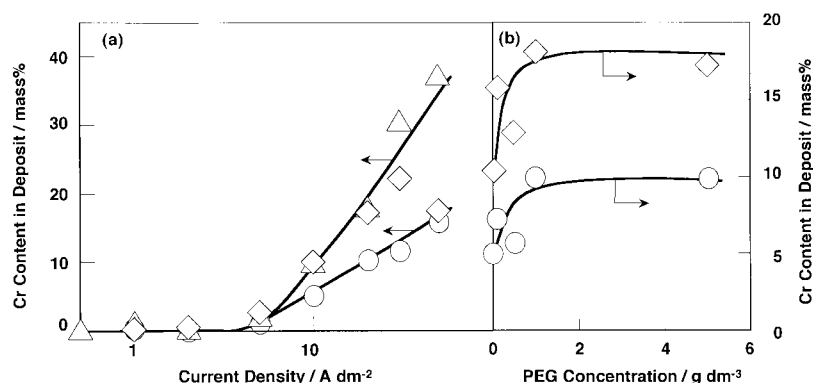


Fig. 1. Effects of current density and PEG concentration in bath on Cr content in deposit. (a) PEG concentration: (○) PEG-free, (△) 1.0 and (◇) 5.0 g dm<sup>-3</sup>; (b) current density: (○) 10 and (◇) 20 A dm<sup>-2</sup>.

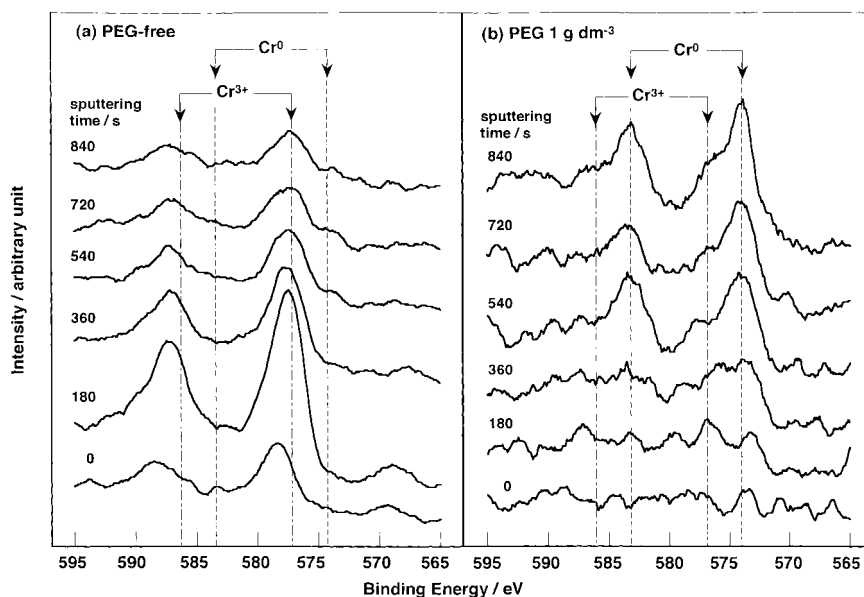


Fig. 2. XPS spectra of Cr in deposit obtained from PEG-free and PEG-containing baths.

when PEG is not present in the baths the hydrolysis products of unreduced chromium(III) are incorporated in the deposited zinc during the electrolysis.

The peaks at the binding energy of metallic chromium appeared on the XPS spectra of the deposits from the PEG-containing baths after a few minutes of argon sputtering. The peak height increased with increase in the sputtering duration, although small peaks of chromium(III) compounds were also observed at the early stages of the sputtering process. Therefore, chromium existed in its metallic state in the bulk deposits to form a zinc–chromium alloy in the presence of PEG in the baths.

Figure 3 shows the effect of PEG addition ( $1.0 \text{ g dm}^{-3}$ ) on the morphology of the deposits obtained at 10 and 20  $\text{A dm}^{-2}$ . The deposits from the PEG-free baths consisted of angular platelets with a size of a few microns. By addition of PEG, the deposits showed more compacted surface and were composed of finer grains. In fact, PEG additions changed the visual appearance of the deposits from dull gray to lustrous.

### 3.2. Effect of mean molecular weight of PEG on alloy deposition

PEG is known to have various molecular weights depending on the degree of polymerization. The effect of the degree of polymerization of PEG on the electro-

deposition behaviour of zinc–chromium alloys was then studied by preparing baths containing PEG of different molecular weights.

Figure 4(a) shows the chromium content in the deposits with respect to the current density when the mean molecular weight of PEG was changed from 200, 4000 to 10 000. In the Figure, the chromium content in the deposits from the PEG-free baths is also shown as a reference. It was found that the chromium content in the deposits increased with increase in the molecular weight of PEG when the current density exceeded 5  $\text{A dm}^{-2}$ . In Fig. 4(b), the chromium content in the deposits was plotted as a function of the molecular weight of PEG. With an increase in the molecular weight of PEG, the chromium content increased first, then became constant when the molecular weight exceeded 1540.

Figure 5 shows the XPS spectra of chromium in the deposits obtained in baths containing PEG of various molecular weights. Chromium in the deposits obtained in the baths containing PEG 1540 and 4000 existed in its metallic state, and chromium(III) was present in the deposits obtained in the PEG-free and PEG 200 containing-baths. Therefore, PEG has no effect on the reduction of chromium(III) ion to its metallic state when the molecular weight is small. Figure 6 shows the effect of molecular weight of PEG on the morphology of the deposits. The deposits obtained in the PEG 200

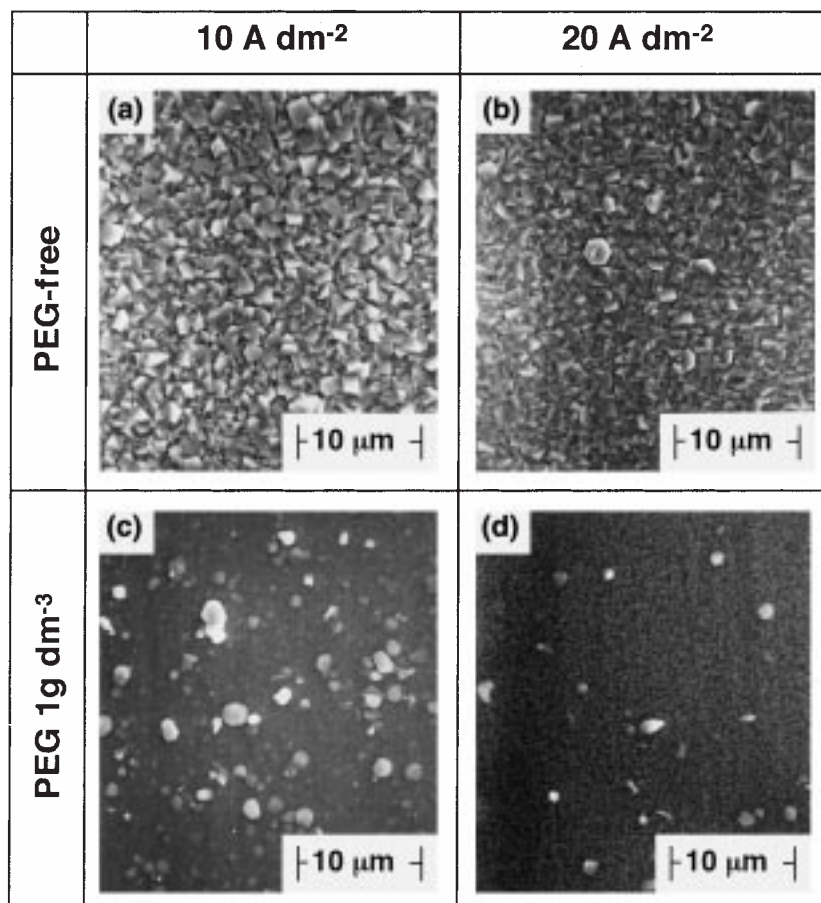


Fig. 3. Effect of PEG on morphology of deposit obtained at 10 and 20  $\text{A dm}^{-2}$ .

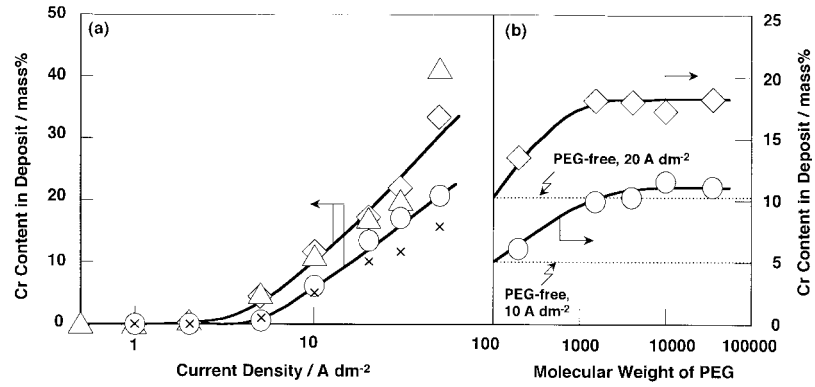


Fig. 4. Effects of current density and molecular weight of PEG on Cr content in deposit. (a) Molecular weight of PEG: (○) 200, (△) 4000, (◇) 10 000 and (×) PEG-free; (b) current density: (○) 10 and (◇) 20 A dm<sup>-2</sup>.

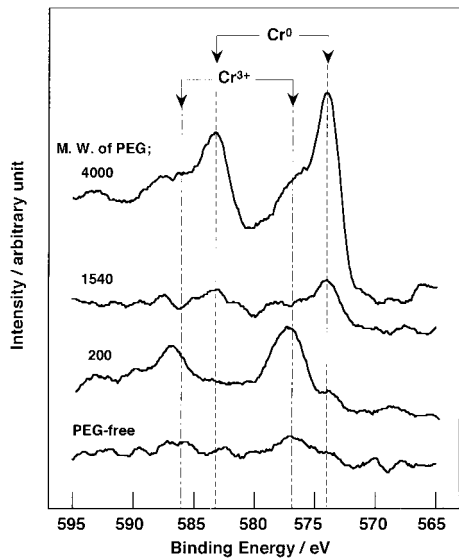


Fig. 5. XPS spectra of Cr in deposits obtained in baths containing PEG with various molecular weights.

containing-baths showed a rough surface which might have resulted from the existence of unreduced chromium(III) compounds. On the other hand, the zinc-chromium alloys with smooth and compact surfaces were electrodeposited from the baths containing PEG 1540 and 4000.

### 3.3. Role of PEG in zinc-chromium alloy deposition

Figure 7 shows the polarization curves for alloy deposition from the bath containing 1.0 g dm<sup>-3</sup> of PEG (1540). Since metallic chromium can be codeposited in this plating condition, the partial polarization curve of chromium together with that of zinc is also presented in this figure. The standard electrode potentials of Cr(III)/Cr(II) and Cr(II)/Cr(0) are -0.61 and -1.11 V vs sat. Ag/AgCl, respectively. The metallic chromium is stable at potentials less positive than -1.1 V and therefore chromium is the less-noble metal than zinc (standard electrode potential Zn(II)/Zn is -0.96 V vs sat. Ag/AgCl). It was found in Figure 7 that the partial polarization curve

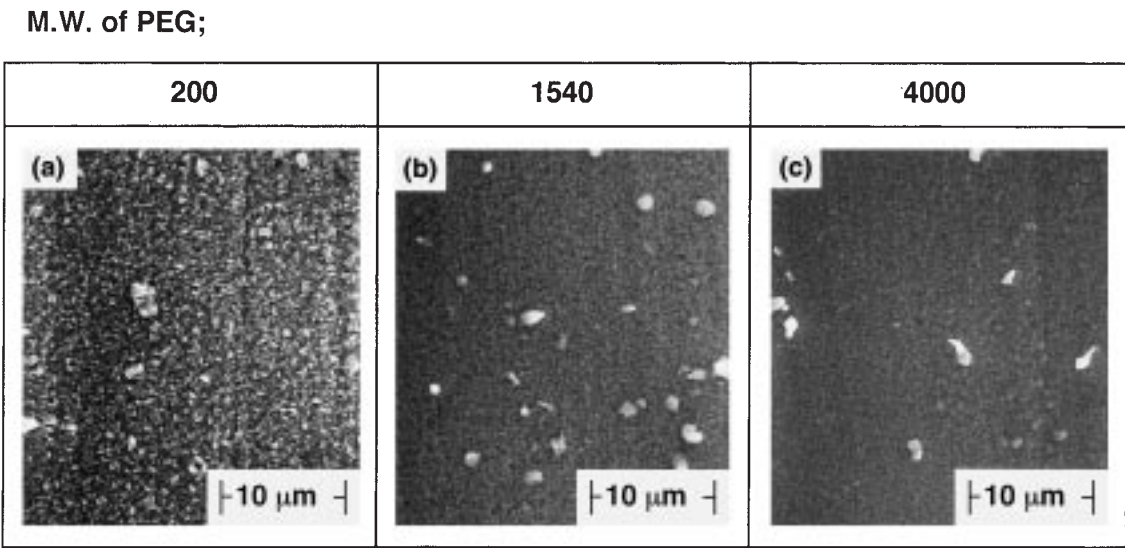


Fig. 6. Effect of molecular weight of PEG on morphology of deposit.

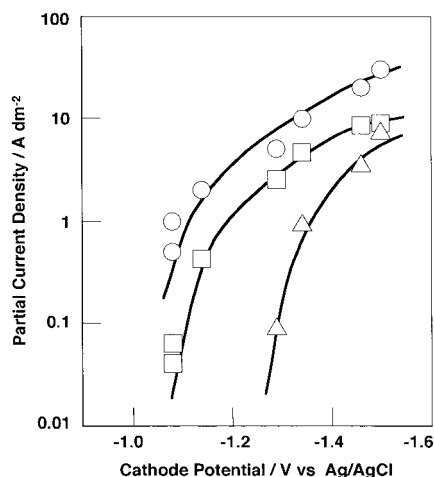


Fig. 7. Polarization curves for alloy deposition from bath containing  $1.0 \text{ g dm}^{-3}$  of PEG (1540). Key: (○) total polarization curve, (□) partial polarization curve of Zn and (△) partial polarization curve of Cr.

of zinc was located in the potential region more positive than that of chromium. Moreover, the composition of the alloy estimated under diffusion control of both metal ions is about 38 mass% chromium. The chromium content in the deposits in this experiment was always less than 40 mass %, and, therefore, zinc is electrodeposited in preference to chromium. According to Brenners's criteria [21], this suggests that the codeposition behaviour of zinc–chromium alloys from the sulfate baths can be classified as a regular type.

Figure 8 shows the effect of the concentration and the molecular weight of PEG on the cathode potential at a current density of  $5.0 \text{ A dm}^{-2}$  above which chromium codeposition is observed. The cathode potential was abruptly shifted to a less positive direction and became constant with increase in concentration and molecular weight of PEG. By taking into account previous XPS results (Figures 2 and 5), it is found that the cathode potential at which metallic chromium begins to codeposit is around  $-1.3 \text{ V}$ .

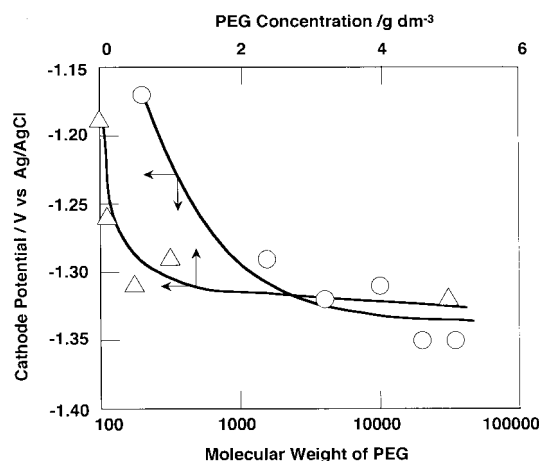


Fig. 8. Effects of concentration and molecular weight of PEG on cathode potential at  $5.0 \text{ A dm}^{-2}$ .

Figure 9 shows the partial polarization curves of zinc in the electrodeposition of zinc–chromium alloys from the PEG-free and PEG-containing baths. In the PEG-free and the PEG 200-containing baths, zinc deposited around the standard electrode potential of zinc ( $-0.96 \text{ V}$  vs sat. Ag/AgCl). However, with increase in the molecular weight and concentration of PEG, the partial polarization curves of zinc were shifted in a less positive direction. Thus a suppressed rate of zinc deposition was observed in the presence of PEG with a higher molecular weight. On the other hand, the partial polarization curves of chromium were not affected by the concentration and molecular weight of PEG, when metallic chromium was codeposited.

It is well known that zinc begins to electrodeposit at its equilibrium potential and little activation overpotential is necessary for its deposition from aqueous sulfate baths. Therefore, it is generally difficult to reach the cathode potential where chromium is reduced to its metallic state (less than  $-1.3 \text{ V}$ ). When the electrodeposition is conducted at higher current densities than the

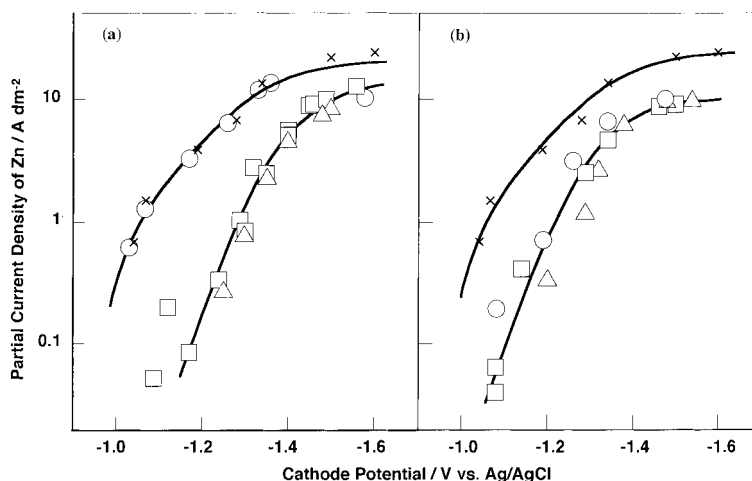


Fig. 9. Effects of molecular weight and concentration of PEG on partial polarization curve of Zn. (a) Molecular weight of PEG: (○) 200, (□) 4000, (△) 10 000 and (×) PEG-free; (b) PEG concentration: (○) 0.1, (□) 1.0 and (△)  $5.0 \text{ g dm}^{-3}$  and (×) PEG-free.

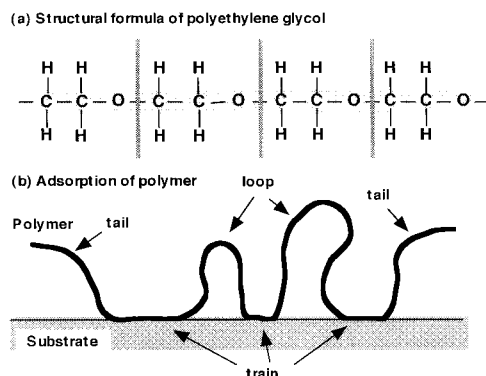


Fig. 10. Molecular structural formula of polyethylene glycol (a) and schematic illustration of adsorbed polymer on substrate (b). Reproduced from [24].

limiting current density of zinc, the reduction potential to metallic chromium can be attained. However, the deposits obtained under diffusion control are powdery and unfavorable for practical use. Accordingly, it can be concluded that the role of PEG in the zinc–chromium alloy deposition is to polarize the zinc deposition (as well as hydrogen evolution) to a less positive region, which permits the codeposition of metallic chromium with zinc.

The polarization effect of PEG may be attributed to the adsorption of PEG on the active sites for metal deposition [22]. Figure 10 shows the structural formula of PEG and the schematic illustration of the adsorption of polymers on the substrate surface. In the case of polymer adsorption, the saturated amount of adsorbed polymer is known to increase with increase in molecular weight [23]. By addition of PEG of higher molecular weight, the suppression of zinc deposition was definitely observed, while PEG with smaller molecular weight showed little effect on the alloy deposition. Therefore, PEG seems to adsorb in the same manner as shown in Figure 10 and enables the codeposition of metallic chromium with zinc.

#### 4. Conclusion

The effect of PEG on the electrodeposition of zinc–chromium alloys was investigated in trivalent chromium baths. The chromium content in the deposits increased with increase in the concentration and molecular weight of PEG. The addition of PEG with molecular weight higher than 1540 permitted the deposition of zinc–chromium alloys of smooth and lustrous surfaces, while no deposits containing metallic chromium were

obtained in the PEG-free baths and the baths containing PEG with lower molecular weight. The cathode potential was shifted in the less positive direction with increase in concentration and molecular weight of PEG. Therefore, PEG inhibits zinc deposition by adsorbing on the cathode, thus making it possible to attain the deposition potential of metallic chromium.

#### References

1. T. Asamura, Proceedings of the 4th International Conference on 'Zinc and Zinc Alloy Coated Steel Sheet', Makuhari, Japan (1998), p. 14.
2. H.E. Townsend, D.D. Davidson and M.R. Ostermiller, Proceedings *op. cit.* [1], p. 659.
3. A. Fukada, K. Arai, S. Suzuki and T. Kanamaru, *CAMP-ISIJ* **4** (1991) 1602.
4. S. Suzuki, T. Kanamaru, K. Arai and A. Fukada, *CAMP-ISIJ* **4** (1991) 68.
5. A. Takahashi, Y. Miyoshi and T. Hada, *J. Surf. Finish. Jpn.* **45** (1994) 301.
6. M.R. El-Sharif, Y.J. Su, A. Watson and C.U. Chisholm, Proc. 80th AESF Annual Conference (1993), p. 1083.
7. A. Watson, Y.J. Su, M.R. El-Sharif and C.U. Chisholm, *Trans. Inst. Met. Finish.* **71**(1) (1993) 15.
8. J.C. Crowther and S. Renton, *Electroplat. Met. Finish.* **28**(5) (1975) 6.
9. C. Barnes, J.J.B. Ward and J.R. House, *Trans. Inst. Met. Finish.* **55**(2) (1977) 73.
10. S. Kato, S. Goto and S. Konishi, *J. Met. Finish. Jpn.* **28** (1977) 121.
11. D.J. Barclay, T.E. Such and J.M.L. Vigar, Proceedings of the 10th World Congress on 'Metal Finishing', Kyoto, Japan (1980), p. 79.
12. D. Smart, T.E. Such and S.J. Wake, *Trans. Inst. Met. Finish.* **61**(3) (1983) 105.
13. D.L. Snyder, Proceedings of the 80th AESF Annual Technology Conference, Session K (1993), p. 445.
14. N. Zaki, Proceedings *op. cit.* [13], Session K, (1993), p. 461.
15. P.J. Elving and B. Zemel, *J. Am. Chem. Soc.* **79** (1957) 1281.
16. H. Stünzi, L. Spiccia, F. Rotzinger and W. Marty, *Inorg. Chem.* **28** (1989) 66.
17. A. Watson, A.M.H. Anderson, M.R. El-Sharif and C.U. Chisholm, *Trans. Inst. Met. Finish.* **69**(1) (1991) 26.
18. A.M. Smith, A. Watson and D.H. Vaughan, *Trans. Inst. Met. Finish.* **71**(3) (1993) 106.
19. M.R. El-Sharif, S. Ma, C.U. Chisholm and A. Watson, Proceedings of the 80th AESF Annual Technology Conference, Session K (1993), p. 451.
20. Z. Tu, Z. Yang, J. Zhang, M-Z. An and W-L. Li, *Plat. Surf. Finish.* **80**(11) (1993) 79.
21. A. Brenner, 'Electrodeposition of Alloys', 1, 2 (Academic Press, 1963).
22. J.P. Healy and D. Pletcher, *J. Electroanal. Chem.* **338** (1992) 155.
23. M. Kawaguchi, K. Hayakawa and A. Takahashi, *Polymer J.* **12** (1980) 265.
24. A. Takahashi and M. Kawaguchi, *J. Society of Rubber Industry, Jpn* **60** (1987) 231.